JCTC Journal of Chemical Theory and Computation

Assessment of Density Functionals for Intramolecular Dispersion-Rich Interactions

Tanja van Mourik*

School of Chemistry, University of St. Andrews, North Haugh Fife KY16 9ST, Scotland, U.K.

Received June 19, 2008

Abstract: A range of density functional theory methods, including conventional hybrid and meta-hybrid functionals, a double-hybrid functional, and DFT-D (DFT augmented with an empirical dispersion term) were assessed for their ability to describe the three minima along the ϕ_{Gly} rotational profile of one particular Tyr-Gly conformer. Previous work had shown that these minima are sensitive to intramolecular dispersion and basis set superposition error, the latter rendering MP2 calculations with small to medium-sized basis sets unsuitable for describing this molecule. Energy profiles for variation of the ϕ_{Gly} torsion angle were compared to an estimated CCSD(T)/CBS reference profile. The hybrid functionals and the meta-hybrid PWB6K failed to predict all three minima; the meta-hybrid functionals M05−2X and M06−2X and the nonhybrid meta functional M06-L as well as the double-hybrid mPW2-PLYP and the B3LYP-D method did find all three minima but underestimated the relative stability of the two with rotated C-terminus. The best performance was delivered by the most elaborate density functional theory model employed: mPW2-PLYP-D. Only M06−2X and mPW2-PLYP-D predicted the correct order of stability of the three minima.

1. Introduction

Intramolecular interactions with aromatic residues are known to play a crucial role in defining the secondary structure of peptides and proteins.[1] Unfortunately, such interactions are inherently difficult to describe computationally. Interactions involving π-electron clouds are affected by electrostatic as well as dispersion forces, and thus, the computational method must be able to describe these forces accurately. Most well-established density functionals like B3LYP do not describe dispersion forces correctly and are therefore not suitable for studying molecules containing aromatic rings. Unfortunately, second-order Møller−Plesset perturbation theory (MP2), which is the simplest correlated ab initio method, also has problems describing π-interactions correctly: whereas MP2 does describe both electrostatic and dispersion interactions, it produces large intramolecular BSSE (basis set superposition error) values unless very large basis sets are employed.[2−4] We encountered these problems recently while studying the tyrosyl-glycine (Tyr-Gly) dipeptide. MP2 single-point calculations (at B3LYP-optimized geometries) predicted that the six most stable conformers contain a folded "book" conformation, whereas B3LYP favored extended conformers.[5] MP2 geometry optimization of the book conformers significantly changed their geometries, increasing their degree of foldedness and stability relative to extended conformations. Further studies on the two book conformers that changed most dramatically from B3LYP to MP2 geometry optimization, labeled "book4" and "book6" in refs 2 and 3, showed that neither B3LYP nor MP2, when coupled with the medium-sized basis set 6−31+G(d), is able to predict the correct geometry of these conformers.[2,3] For book6, the much more folded structure predicted by MP2 appeared to be entirely an artifact caused by intramolecular BSSE, and for this conformer, B3LYP essentially predicted the correct structure.[3] The situation is slightly more complicated for book4. Here, the B3LYP and MP2 optimized structures mainly differ in the orientation of the C-terminus, as characterized by the ϕ_{Gly} Ramachandran angle (see Figure 1). Potential energy profiles were created by optimizing the

* Corresponding author phone: +44 (0)1334 463822; fax: +44 (0)1334 463808; e-mail: tanja.vanmourik@st-andrews.ac.uk.

10.1021/ct800231f CCC: $40.75
Published on Web 09/13/2008

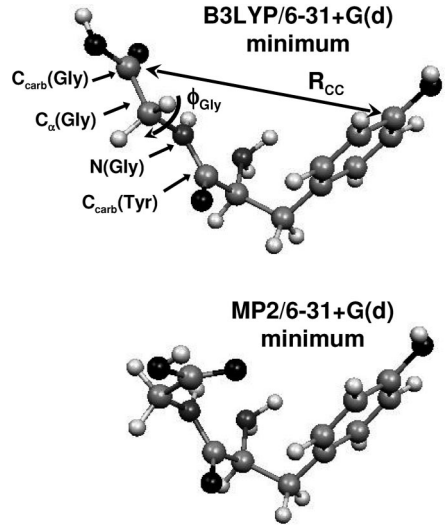

Figure 1. The B3LYP/6−31+G(d) and MP2/6−31+G(d) optimized geometries of the Tyr-Gly conformer book4.

book4 structure for fixed ϕ_{Gly} values.[2] Single-point calculations were performed with df-MP2[6] (density-fitted MP2) and df-LMP2[6−9] (density-fitted local MP2) using large basis sets (aug-cc-pVDZ - aug-cc-pVQZ[10,11]) to reduce the BSSE. The "df" approximation significantly reduces the cost of the two-electron-four-index integrals,[6] thereby allowing the use of much larger basis sets than would be feasible with canonical MP2. The "local" approximation is also designed to reduce computational cost. In addition, this approximation reduces the size of the BSSE.[12−15] The df-(L)MP2 calculations showed that there are three minima along the energy profile. However, neither B3LYP/6−31+G(d) nor MP2/6−31+G(d) found all three minima, which was attributed to intramolecular BSSE in the MP2 calculations and missing dispersion in the B3LYP calculations. Thus, neither is a suitable level of theory to study interactions with π-electron clouds.

Similar problems with intramolecular BSSE have been encountered recently in other systems containing aromatic rings. For example, large intramolecular BSSE effects in MP2 calculations were responsible for predicting the wrong order of stability of the Phe-Gly-Phe tripeptide,[16] whereas a more extreme example of the effect of intramolecular BSSE is provided by the series of [*n*]helicenes.[16] Here, the large number of π-π interactions per benzene ring caused such a large intramolecular BSSE effect in the MP2 calculations that clearly absurd results were obtained.

Evidently, reducing the intramolecular BSSE in MP2 calculations by using very large basis sets readily becomes intractable for large molecular systems. An alternative, computationally more efficient approach may be to make use of recent efforts to include dispersion in density functional theory (DFT). As DFT is much less basis-set dependent than MP2, intramolecular BSSE effects are much smaller. Over the last years, many new functionals have been developed to rectify the deficiencies (in particular, the inability to describe dispersion correctly) of earlier functionals. In the current work we assess a number of modern functionals for their ability to reproduce all three minima in the book4 rotational energy profile. The functionals considered fall into the following categories: hybrid GGA (generalized gradient approximation) functionals, which contain a percentage of exact Hartree−Fock (HF) exchange, and hybrid-meta GGAs, which in addition explicitly depend on the kinetic energy density. We also used one meta-GGA functional (no Hartree−Fock exchange). The hybrid GGAs considered include B3LYP,[17,18] B97−1,[19,20] X3LYP,[21] and BHandH (or BH&H).[22] B3LYP is by far the most popular functional, representing about 80% of the total occurrences in the literature over 1990−2006.[23] B97−1 was found to be among the functionals that gave the best results for a combination of thermochemical kinetics and nonbonded interactions[24,25] and was the best-performing functional without kinetic energy in a study on H-bonded and stacked structures of formic acid tetramers and formamide tetramers.[26] The X3LYP functional was designed for noncovalent interactions.[21] It describes hydrogen bonding accurately[27,28] but was found to fail for stacking interactions.[29] BHandH was found to give good results for dispersion systems but overestimates hydrogen-bonding interactions.[30] The meta-hybrid GGAs considered in this work include PWB6K,[31] M05−2X,[24] and M06−2X,[32] all originating from the Truhlar group. The nonhybrid (local) meta-GGA M06-L[33] also originates from this group. PWB6K was developed for thermochemistry and nonbonded interactions[31] and has consistently shown very good performance for noncovalent interactions.[26,34,35] The M05−2X, M06−2X, and M06-L functionals were developed by Truhlar et al. as part of two suites of functionals, the M05[31,36] and M06[33,37,38] series, intended to yield broad applicability in chemistry. The M06 suite was built on the experience gained with the M05 functionals and essentially supersedes these.[37] M06−2X was shown to perform very well for aromatic−aromatic stacking interactions,[37] though in a recent study on the glycyl-phenylalanyl-alanine peptide this functional failed to reproduce the relative order of stability of sixteen low-lying peptide conformers.[39] M06-L was found to be the only local functional that outperformed B3LYP using a test set including data for main-group thermochemistry, barrier heights, noncovalent interactions, and transition metal chemistry.[37]

We also used a double-hybrid density functional, mPW2-PLYP,[40] which was found to perform very well for weak interactions.[41] Double-hybrid functionals can be seen as a mixture of hybrid DFT and MP2: in addition to mixing in a portion of exact Hartree−Fock exchange (E_X^{HF}), as done in hybrid GGAs, double-hybrid functionals also mix in a fraction of MP2 correlation energy (E_C^{MP2}), calculated with the hybrid DFT orbitals.[42] In the case of mPW2-PLYP, the exchange and correlation functionals E_X^{GGA} and E_C^{DFT} are provided by mPW[43] and LYP,[18] respectively. The total exchange-correlation energy E_{XC} is then given by

$$E_{XC} = (1-a)E_X^{GGA} + aE_X^{HF} + (1-b)E_C^{DFT} + bE_C^{MP2} \quad (1)$$

For mPW2-PLYP, the HF-exchange mixing parameter a and the MP2 correlation mixing parameter b are 0.55 and 0.25, respectively.[40]

An alternative method to overcome the deficiencies of density functionals is to augment the functional with an empirical dispersion term. In this work we have used the

DFT-D method of Grimme,[44,45] where the dispersion energy is described by a damped potential of the form C_6R^{-6}:

$$E_{disp} = -s_6 \sum_{i-1}^{N_{at}-1} \sum_{j=i+1}^{N_{at}} \frac{C_6^{ij}}{R_{ij}^6} f_{dmp}(R_{ij}) \quad (2)$$

Here, N_{at} is the number of atoms, C_6^{ij} is the dispersion coefficient for atom pair ij, s_6 is a global scaling factor only dependent on the density functional used, and R_{ij} is the interatomic distance. The damping function f_{dmp} is given by[44,45]

$$f_{dmp}(R_{ij}) = \frac{1}{1 + e^{-d(R_{ij}/R_r - 1)}} \quad (3)$$

Here, R_r is the sum of the van der Waals radii. For mPW2-PLYP the scaling parameter s_6 and the damping factor d are 0.40 and 20, respectively.[40]

It was shown that Grimme's parametrization yielded interaction energies that deviated on average by less than 10% from reference CCSD(T) values for a benchmark set consisting mainly of DNA base pairs and amino acid pairs.[46] For π-stacked structures DFT-D gave results in good agreement with the reference SCS-MP2 (spin-component-scaled MP2) results.[47,48] However, larger deviations were found for anisole-water and anisole-ammonia, where B3LYP-D yielded overestimated interaction energies with the ammonia or water located too close to the anisole molecule.[49] This was attributed to either an overestimated dispersion correction or to double-counting of electron correlation effects by the DFT and van der Waals parts of the method, which is expected to be worse at short-range distances.

In the current paper we show that the meta functionals (except the older PWB6K) and the double-hybrid functional as well as the DFT-D methods considered clearly outperform the conventional hybrid functionals in describing the Tyr-Gly conformer studied. The overall best agreement with the estimated CCSD(T)/CBS results is provided by the mPW2-PLYP-D method (double-hybrid functional, augmented with an empirical dispersion term).

2. Methodology

2.1. DFT Energy Profiles. The MP2/6−31+G(d) and B3LYP/6−31+G(d) geometries of the Tyr-Gly conformer book4 mainly differ in the orientation of the C-terminus, as characterized by the Ramachandran angle ϕ_{Gly} (equaling the C_{carb}(Tyr)-N(Gly)-C_α(Gly)-C_{carb}(Gly) dihedral angle – see Figure 1). Energy profiles for rotation around the glycine N(Gly)-C_α(Gly) bond were determined by single-point energy calculations at structures with ϕ_{Gly} values ranging from 40−310°. These structures were obtained by geometry optimization at fixed ϕ_{Gly} values at the M05−2X/6−31+G(d) level of theory. The relative energies used to create the energy profiles were computed relative to the energy of the conformer with $\phi_{Gly} = 180°$. The profiles were computed with the B3LYP,[17,18] B97−1,[19,20] X3LYP,[21] Gaussian's version of Becke's half-and-half functional BHandH,[22] mPW2-PLYP,[40] PWB6K,[31] M05−2X,[24] M06−2X,[32] M06-L,[33] B3LYP-D,[44,45] and mPW2-PLYP-D[50] density functional methods. The M05−2X profiles were computed with the 6−31+G(d),[51−53] aug-cc-pVDZ, and aug-cc-pVTZ[10,11] basis sets. All other DFT profiles were calculated with aug-cc-pVDZ only. The X3LYP, B97−1, and BHandH calculations were done with Gaussian 03,[54] the PWB6K, M05−2X, M06−2X, and M06-L calculations were done with NWChem,[55] whereas the mPW2-PLYP, mPW2-PLYP-D, B3LYP, and B3LYP-D calculations were performed with ORCA.[56] The mPW2-PLYP calculations invoked the RI (resolution of the identity) approximation (similar to the density-fitting approach) for the MP2 part, using automatic generation of a general-purpose fitting basis set. The B3LYP calculations employed the VWN1[57] correlation functional (Gaussian's definition of the B3LYP functional). The Gaussian calculations used the "UltraFine" integration grid (containing 99 radial shells and 590 angular points per shell), the NWChem calculations employed the "xfine" grid (125 radial and 1454 angular shells), and the ORCA calculations employed "grid 6" (default GaussChebyshev radial grid coupled with 590 angular Lebedev points).

2.2. The Reference Profile. Single-point df-LMP2[6−9] calculations were performed at the M05−2X/6−31+G(d) geometries using the aug-cc-pVDZ and aug-cc-pVTZ basis sets. The corresponding aug-cc-pVDZ-MP2fit and aug-cc-pVTZ-MP2fit fitting basis sets[58] were used for both the df-HF and df-LMP2 parts of the calculation. The profiles were also computed with df-HF/aug-cc-pVQZ, whereas df-MP2 and df-LMP2 calculations with the aug-cc-pVQZ/aug-cc-pVQZ-MP2fit basis set combination were carried out for selected geometries only (ϕ_{Gly} = 80, 130, 180, 240, and 285°). In the local calculations all pairs were treated as strong pairs, as recommended to avoid discontinuities on the potential energy surface due to orbital domain changes.[59,60] In addition, single-point calculations with df-LCCSD-(T0)[12,61−63] (density-fitted local coupled cluster with single, double and perturbative noniterative local triple excitations) were performed with the aug-cc-pVDZ/aug-cc-VDZ-MP2fit basis set combination. Df-LCCSD(T0) calculations with aug-cc-pVTZ/aug-cc-pVTZ-MP2fit were done for $\phi_{Gly} = 180$ and 285°, to provide a one-point test of the $E_{CCSD(T)corr}$/aug-cc-pVDZ higher-order correlation correction term (see below). The default selection of the pair classes was used. In the df-LMP2 and df-LCCSD(T0) calculations the two most diffuse functions of each angular momentum function were ignored in the localization to yield better-localized orbitals. A completion criterion of 0.99 was employed for the orbital domain selection. Despite treating all pairs as strong pairs in the LMP2 calculations, at some points along the df-LMP2 and df-LCCSD(T0) profiles the orbital domains changed slightly, leading to steps in the potential energy curve. We redid those calculations using the same orbital domains as used for $\phi_{Gly} = 180°$, except in the case of df-LMP2/aug-cc-pVQZ, where the orbital domains of $\phi_{Gly} = 80°$ were used, as these were the same as those of ϕ_{Gly} = 130, 240, and 285° (i.e., only the 180°-domains were different). The df-LMP2 and df-LCCSD(T0) calculations were done with Molpro 2006.[64]

Complete basis set (CBS) CCSD(T) limits were estimated as follows: the aug-cc-pVDZ and aug-cc-pVTZ df-LMP2 correlation energies, and for selected geometries also the aug-

cc-pVTZ/aug-cc-pVQZ correlation energies, were extrapolated to the CBS limit using the two-point extrapolation scheme of Halkier et al.[65]

$$E_{\mathrm{MP2correl,CBS}} = \frac{X^3}{X^3-(X-1)^3}E_{\mathrm{correl},X} - \frac{(X-1)^3}{X^3-(X-1)^3}E_{\mathrm{correl},X-1} \quad (4)$$

Here, X is the cardinal number of the largest basis set used in the extrapolation ($X = 3$ for aug-cc-pVDZ/aug-cc-pVTZ extrapolation; $X = 4$ for aug-cc-pVTZ/aug-cc-pVQZ extrapolation). The extrapolated correlation energy contributions were then added to the df-HF/aug-cc-pVQZ total energies. A higher-order correlation correction term, $E_{\mathrm{CCSD(T)corr}}$, was added by calculating the difference between the df-LMP2 and df-LCCSD(T0) total energies computed with the aug-cc-pVDZ basis set. It was shown previously that the basis set dependence of the CCSD(T) correction term for interaction energies is small,[66−68] and therefore, the aug-cc-pVDZ basis set should give an accurate estimate of the higher-order correlation correction.

Thus, the total energies required for the estimated CCSD(T)/CBS reference profile were computed as

$$E_{\mathrm{CCSD(T)/CBS}} = E_{\mathrm{HF}}(\mathrm{avqz}) + E_{\mathrm{MP2correl,CBS}}(\mathrm{avdz/avtz}) + E_{\mathrm{CCSD(T)corr}}(\mathrm{avdz}) \quad (5)$$

where avnz (n = d, t, q) is an abbreviated notation for aug-cc-pVnZ (n = D, T, Q). As above, the relative energies for the CCSD(T)/CBS profile were computed relative to the value at $\phi_{\mathrm{Gly}} = 180°$.

3. Results

3.1. The B3LYP/6−31+G(d) and MP2/6−31+G(d) Profiles. In previous work we had found that B3LYP/6−31+G(d) geometry optimization predicted an extended structure of the Tyr-Gly conformer book4, with a ϕ_{Gly} angle of 180°, whereas MP2/6−31+G(d) geometry optimization yielded a more folded structure, with a ϕ_{Gly} angle of 74°.[5] Figure 1 contrasts the B3LYP and MP2 optimized structures. The MP2 structure is more compact, with closer contact between the glycine/C-terminus and the tyrosine aromatic ring. In further work on this molecule, relaxed potential energy profiles at fixed values of ϕ_{Gly}, computed at these two levels of theory, were compared to the profile computed with df-LMP2/aug-cc-pVTZ.[2] These profiles, constructed from the work presented in ref 2, are shown in Figure 2. The df-LMP2/aug-cc-pVTZ method is expected to give the correct profile, as it is nearly BSSE-free, describes dispersion, and was found to produce relative energies in close agreement with df-LCCSD(T0) results for the Tyr-Gly conformer book6[3] (indicating that a possible overestimation of dispersion by the MP2 method, as is often seen in stacking and other weakly bound interactions,[69] is very small for this molecule).

The df-LMP2/aug-cc-pVTZ profile, displayed in Figure 2, clearly shows three minima at roughly 80, 180, and 280°. The minimum at 80° is the global minimum, whereas the 280°-minimum is shallowest. The MP2/6−31+G(d) profile reproduces the minima at 80 and 280° but completely misses the 180°-minimum. In previous work we showed that this is due to large intramolecular BSSE effects in the MP2/6−31+G(d) calculations.[2] In contrast, the B3LYP profile only shows the minimum at 180°. The other two minima are absent, presumably due to missing dispersion in the B3LYP calculations.

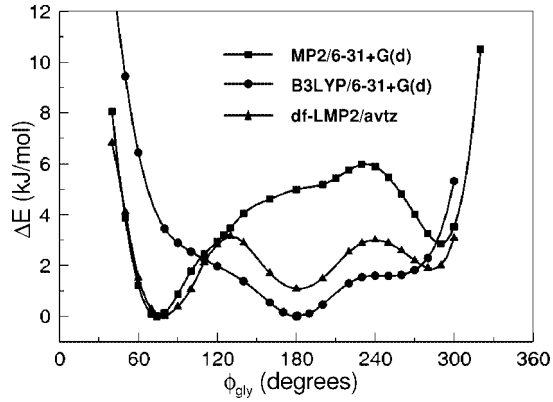

Figure 2. B3LYP/6−31+G(d), MP2/6−31+G(d), and df-LMP2/avtz potential energy profiles for rotation around the ϕ_{Gly} N(Gly)-C_α(Gly) bond (avtz = aug-cc-pVTZ). The B3LYP profile used structures optimized with B3LYP/6−31+G(d) at fixed ϕ_{Gly} angles. The MP2 and df-LMP2 profiles were computed using structures optimized with MP2/6−31+G(d) at fixed ϕ_{Gly} angles. The minimum energy points in the profiles (B3LYP: $\phi_{\mathrm{Gly}} = 180°$; MP2: $\phi_{\mathrm{Gly}} = 74°$; df-LMP2: $\phi_{\mathrm{Gly}} = 80°$) were taken as the reference point for the relative energies.

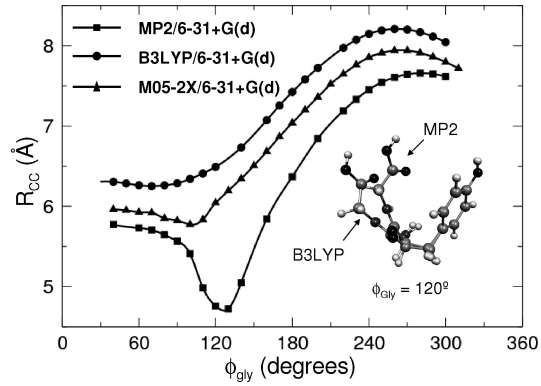

Figure 3. Variation of the R_{CC} distance as a function of the ϕ_{Gly} torsion angle in the partially optimized structures obtained with B3LYP/6−31+G(d), MP2/6−31+G(d), and M05−2X/6−31+G(d). The inset shows a comparison of the B3LYP and MP2 geometries at $\phi_{\mathrm{Gly}} = 120°$.

3.2. Tyr-Gly Geometries along the Energy Profile. In our previous work,[2] the B3LYP profile was computed using partially optimized structures (at fixed values of ϕ_{Gly}) obtained with B3LYP/6−31+G(d), whereas the MP2 and df-LMP2 profiles used the partially optimized MP2/6−31+G(d) geometries. However, the MP2 and B3LYP structures differ to some extent. In the MP2 structures the glycine/C-terminus chain is closer to the tyrosine ring, as exemplified by the distance R_{CC} between the C_{carb}(Gly) and tyrosine C(OH) atoms, shown in Figure 3. Over the whole ϕ_{Gly} range the R_{CC} distances are shorter in the MP2 structures

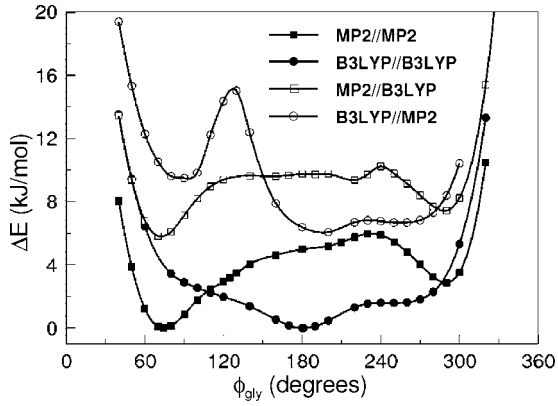

Figure 4. B3LYP/6−31+G(d) and MP2/6−31+G(d) potential energy profiles for rotation around the N(Gly)-C_α(Gly) bond, using the B3LYP/6−31+G(d) and MP2/6−31+G(d) sets of geometries. In "Method1//Method2" Method1 is the method used for the calculation of the single-point energies, whereas Method2 is the method used to obtain the geometries. The minimum energy points in the profiles (B3LYP//B3LYP: $\phi_{Gly} = 180°$; MP2//MP2: $\phi_{Gly} = 70°$) were taken as the reference point for the relative energies.

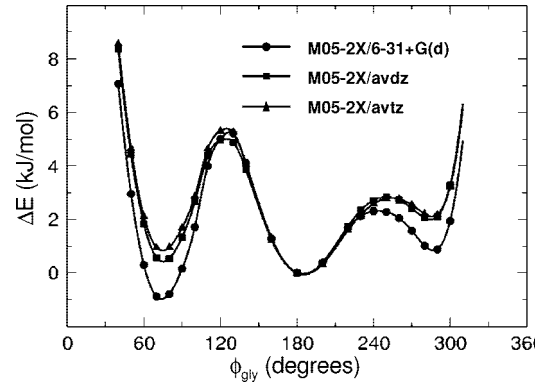

Figure 5. M05−2X potential energy profiles for rotation around the N(Gly)-C_α(Gly) bond computed with the 6−31+G(d), aug-cc-pVDZ (avdz), and aug-cc-pVTZ (avtz) basis sets, using the MP2/6−31+G(d) set of geometries. The energy at $\phi_{Gly} = 180°$ was taken as the reference point for the relative energies.

than in the B3LYP structures. The MP2 R_{CC} profile shows a deep dip around $\phi_{Gly} = 120-130°$, and it is in this region that the MP2 and B3LYP structures differ most. The more compact MP2 structures in this region are likely a result of intramolecular BSSE, which was previously shown to exhibit a sharp peak around 120°.[2]

Figure 4 shows that the shape of the B3LYP and MP2 profiles depends on the set of partially optimized geometries (MP2 or B3LYP) used. Naturally, the B3LYP geometries are not ideal for the MP2 calculations and vice versa, as can be seen by the upward shift of the curves that use the other method's geometries. The shapes of the two MP2 profiles do not differ much, though the profile using the MP2 geometries is more energetically favorable than the one using the B3LYP geometries in the region around 120°, presumably due to the more compact structures predicted by MP2 in this region. The two B3LYP profiles, however, differ considerably. The 180°-minimum in the profile using the B3LYP geometries has shifted toward ∼200° in the profile using the MP2 geometries and has become shallower. The B3LYP profiles differ most dramatically in the region around 100−130°. The profile using the MP2 geometries now exhibits a second minimum at ∼90° with a large barrier separating the 90- and 200°-minima. The greater compactness of the MP2 structures in the region around 120° (cf. Figure 3) clearly leads to less favorable B3LYP energies, pushing up the curve around 120° and thereby creating the 90°-minimum. The MP2 energies appear less dependent on the compactness of the geometries, possibly because any repulsive energy contributions due to conformational strain or repulsive interactions between close atoms in the more compact structures (present in the MP2 as well as B3LYP calculations) are more than compensated by intramolecular dispersion and/or BSSE (mostly absent in the B3LYP calculations). The difference profile of the two B3LYP curves has a shape closely resembling the difference profile of the R_{CC} distances in the MP2 and B3LYP structures, indicating that the shorter R_{CC} distances in the MP2 structures are directly responsible for the large changes in the B3LYP profile (Figure S1, Supporting Information).

The Tyr-Gly geometries should preferentially be optimized using a (virtually) BSSE-free method that also describes dispersion. The B3LYP structures are probably not folded enough due to missing dispersive attraction, whereas the MP2 geometries are likely too compact due to BSSE. As we encountered problems performing partial geometry optimizations with df-LMP2 using Molpro, we instead reoptimized the Tyr-Gly geometries at fixed ϕ_{Gly} torsion angles with M05−2X/6−31+G(d) using NWChem. The M05−2X functional was shown to give a benzene-methane binding energy curve in excellent agreement with CCSD(T),[32] whereas MP2 overestimated the strength of the complex and B3LYP gave a repulsive potential. We therefore expect M05−2X to give reliable geometries for the Tyr-Gly book conformers. Figure 3 shows that the M05−2X geometries are more compact than the B3LYP geometries (as expected from the presence of dispersion) but do not show the sharp increase in compactness around 120−130° as exhibited by the MP2 structures (which is likely due to BSSE). The geometries therefore appear very plausible. Unless stated otherwise, all subsequent results were obtained using the M05−2X/6−31+G(d) geometries.

3.3. Basis Set Convergence of the M05−2X Profile. Figure 5 shows M05−2X profiles computed with three different basis sets, using the MP2/6−31+G(d) geometries. All profiles nicely show three minima, demonstrating the functional's superiority compared to B3LYP. The 6−31+G(d) basis set appears to overestimate the stability of the minima at ∼80° and ∼280°, as compared to the results obtained with the larger basis sets. The aug-cc-pVDZ and aug-cc-pVTZ curves are very similar, indicating that the results are essentially converged at the aug-cc-pVDZ basis set level. The remainder of this study therefore employed the aug-cc-pVDZ basis set.

3.4. The CCSD(T) Reference Profile. The CCSD(T) reference profile was obtained from the total energies computed according to eq 4, using the M05−2X/6−31+G(d) geometries. The reference profile has four main sources of

Table 1. Comparison of the Relative Energies (in kJ/mol) of Key Structures Computed at Different Levels of Theory[a]

	ϕ_{Gly} (in deg)			
method	80	130	240	285
df-HF/avdz	5.44	3.29	3.03	2.04
df-HF/avtz	6.13	3.29	2.90	2.53
df-HF/avqz	6.33	3.26	2.86	2.53
df-LMP2/avdz	−1.04	1.75	2.21	0.31
df-LMP2/avtz	−1.10	1.55	2.00	0.88
df-LMP2/avqz	−1.00	1.50	2.00	1.04
LMP2/CBS(avdz/avtz)[b]	−1.22	1.43	1.93	0.92
LMP2/CBS(avtz/avqz)[c]	−1.06	1.49	2.03	1.15
MP2/CBS(avtz/avqz)[d]	−1.24	1.60	2.17	1.37
df-LCCSD(T0)/avdz	−1.36	1.65	2.12	−0.29
df-LCCSD(T0)/avtz	—	—	—	0.46
LCCSD(T0)/CBS(avdz/avtz)[e]	−1.54	1.34	1.85	0.32
LCCSD(T0)/CBS(avtz/avqz)[f]	−1.38	1.39	1.94	0.55

[a] The energy at $\phi_{Gly} = 180°$ is taken as the reference point for the relative energies; avdz = aug-cc-pVDZ, avtz = aug-cc-pVTZ, and avqz = aug-cc-pVQZ. The "df" designation is omitted from the CBS entries, as the density fitting approximation should not affect the estimated CBS limits noticeably. [b] LMP2/CBS limit estimated by adding to the df-HF/aug-cc-pVQZ energies the df-LMP2 correlation energy extrapolated using the aug-cc-pVDZ and aug-cc-pVTZ values. [c] LMP2/CBS limit estimated by adding to the df-HF/aug-cc-pVQZ energies the df-LMP2 correlation energy extrapolated using the aug-cc-pVTZ and aug-cc-pVQZ values. [d] MP2/CBS limit estimated by adding to the df-HF/aug-cc-pVQZ energies the df-MP2 correlation energy extrapolated using the aug-cc-pVTZ and aug-cc-pVQZ values. [e] LCCSD(T0)/CBS limit estimated by adding the CCSD(T) correction term, computed with aug-cc-pVDZ, to the LMP2/CBS (avdz/avtz) energies. [f] LCCSD(T0)/CBS limit estimated by adding the CCSD(T) correction term, computed with aug-cc-pVDZ, to the LMP2/CBS (avtz/avqz) energies.

uncertainty: (i) the degree of basis-set convergence of the HF/aug-cc-pVQZ energies, (ii) the accuracy of the aug-cc-pVDZ/aug-cc-pVTZ extrapolation of the MP2 correlation energies, (iii) the accuracy of the CCSD(T) higher-order correlation correction term, and (iv) the accuracy of the local approximation. Errors due to the density fitting approximation are essentially negligible.[6]

Comparison of the df-HF energy profiles computed with aug-cc-pV(D/T/Q)Z shows that the aug-cc-pVDZ basis set slightly overestimates the relative stability of the 80- and 285°-minima (Figure S2a, Supporting Information). However, the aug-cc-pVTZ and aug-cc-pVQZ profiles are very similar (relative energy differences between 0.1−0.4 kJ/mol for ϕ_{Gly} in the 40−100° and 285−310° intervals and nearly 0 kJ/mol in the 100−285° range), indicating that the aug-cc-pVQZ energies are sufficiently converged with respect to the basis set quality. Note that the smaller relative energy differences in the midregion are a direct result of our choice to position the profiles at 0 kJ/mol for $\phi_{Gly} = 180°$. The close similarity of the aug-cc-pVTZ and aug-cc-pVQZ results can also be deduced from the relative energies of the minimum- and maximum-energy points (80, 130, 180, 240, and 285°) along the profile listed in Table 1. These are indicative of the relative stability of the three minima and of the barriers between them. Differences between aug-cc-pV5Z and aug-cc-pVQZ energies would probably be roughly half of those between aug-cc-pVQZ and aug-cc-pVTZ, so that the HF/aug-cc-pVQZ relative energies are estimated to be accurate within ∼0.2 kJ/mol (for $\phi_{Gly} = 40-60°$) and considerably more accurate for larger ϕ_{Gly} angles. The HF/aug-cc-pVQZ relative energies of the 80- and 285°-minima are estimated to be too small by approximately 0.14 and 0.04 kJ/mol, respectively.

Due to the large amount of computational resources required for df-LMP2/aug-cc-pVQZ calculations, these were only performed for the minimum- and maximum-energy points (Table 1). Df-LMP2/aug-cc-pVDZ significantly overestimates the relative stability of the 285°-minimum (see also Figure S2b, Supporting Information). Extrapolation to the CBS limit (using the aug-cc-pVDZ and aug-cc-pVTZ energies) remedies this: the avdz/avtz-extrapolated relative energy of the 285°-structure is almost identical to that computed with df-LMP2/aug-cc-pVQZ. Reassuringly, the CBS(avdz/avtz) and CBS(avtz/avqz) results are very close to each other (differences of at most 0.2 kJ/mol for the minimum and maximum points). Also note that the same overestimation of the relative stability of the 285°-minimum by aug-cc-pVDZ occurs for the df-LCCSD(T0) method (Table 1). The df-LCCSD(T0) relative energy changes from a negative value (−0.29 kJ/mol) when computed with aug-cc-pVDZ to a positive value (0.46 kJ/mol) computed with aug-cc-pVTZ. We estimate that the CBS limits are accurate within ∼0.2 kJ/mol. Based on the differences between the avdz/avtz and avtz/avqz extrapolated results, the avdz/avtz extrapolation likely overestimates the relative stability of the 80- and 285°-minima by approximately 0.2 and 0.12 kJ/mol, respectively.

Sinnokrot and Sherrill found that the CCSD(T) correlation correction term for interaction energies is rather insensitive to the basis set size, as long as the basis set contains diffuse functions.[67] Thus, for the three different benzene dimer configurations (sandwich, T-shaped, and parallel-displaced), the correction term differed by less than 0.2 kJ/mol for the aug-cc-pVDZ or aug-cc-pVTZ(-f/-d) basis sets. Jurečka and Hobza found larger differences (between 0.2 and 0.5 kJ/mol) for CCSD(T) correction terms computed with aug-cc-pVDZ and cc-pVTZ, for dimers consisting of formamide and formamidine units.[66] However, the cc-pVTZ results are expected to be less accurate than the aug-cc-pVDZ ones (because of lacking diffuse functions in cc-pVTZ), so that the larger differences between the correction terms computed with these two basis sets are probably mainly due to errors in the cc-pVTZ rather than in the aug-cc-pVDZ values. To assess the accuracy of the $E_{CCSD(T)corr}$ term for the current molecule, we recomputed with aug-cc-pVTZ its contribution to the relative energy of the conformer with $\phi_{Gly} = 285°$ (which is the conformer minimum with the largest $E_{CCSD(T)corr}$ correction term). The difference between the $E_{CCSD(T)corr}$/aug-cc-pVDZ and $E_{CCSD(T)corr}$/aug-cc-pVTZ contribution to the relative energy of this structure is only 0.18 kJ/mol. In agreement with the results of Sinnokrot and Sherrill, we therefore estimate the aug-cc-pVDZ correction terms to be accurate within ∼0.2 kJ/mol. The $E_{CCSD(T)corr}$/aug-cc-pVDZ correction likely overestimates the relative stability of the 80- and 285°-minima by approximately 0.1 and 0.2 kJ/mol, respectively.

The error introduced by the local approximation cannot be simply deduced from the differences in the local and canonical energies calculated with finite basis sets, as these are partially caused by the much reduced BSSE in the local

calculations. In previous work we showed that df-MP2/aug-cc-pVTZ calculations on the book4 conformer produce large BSSE values of 5−6 kJ/mol, and even with the aug-cc-pVQZ basis set the BSSE still amounts to 2−3 kJ/mol.[2] However, when employing the local approximation the BSSE is below 1 kJ/mol already for the aug-cc-pVTZ basis set. Thus, the local energies may in fact be more reliable than the corresponding nonlocal energies, unless very large basis sets are employed. However at the CBS limit the BSSE is nonexistent, and we therefore estimated the error of the local approximation by comparing the MP2/CBS and LMP2/CBS limits (see Table 1). Relative to the 180°-minimum, the df-LMP2 method slightly overestimates the relative stability of the 285°-structure (by 0.18 kJ/mol), whereas the relative stability of the 80°-structure is slightly underestimated (by 0.22 kJ/mol). The local error in the $E_{CCSD(T)corr}$ term is likely much smaller, due to expected cancelation of errors in the df-LMP2 and df-LCCSD(T0) results.

From this analysis, we expect the reference relative stabilities of the 80°- and 285° minima to be overestimated by approximately 0.3 and 0.6 kJ/mol, respectively.

3.5. Performance of Density Functionals. Figure 6 shows the profiles computed with the different density functional theory methods considered in this work. None of the hybrid functionals yields the correct profile shape (Figure 6a). BHandH finds a minimum around 70°; B3LYP, X3LYP, and B97−1 show a very shallow minimum around 90°; but all hybrid functionals miss the 280°-minimum. The meta functionals perform much better (Figure 6b). The PWB6K profile does not show a minimum in the 280° area, but the M05 and M06-type functionals tested, including the local M06-L functional, nicely predict three minima along the profile, though the relative stability of the 80°- and 280°-minima are underestimated as compared to the reference profile. Only M06−2X predicts the 80°-minimum to be the most stable of the three minima, in agreement with the reference profile. However, the barrier between the 80°- and 180°-minima is much overestimated. The double-hybrid mPW2-PLYP functional and B3LYP-D also underestimate the relative stability of the 80°- and 280°-minima, but the overestimation of the barrier heights is less severe than for the meta functionals (Figure 6c). The mPW2-PLYP-D method performs best, particularly in the 60−240° region. It has been shown that for dispersion complexes double-hybrid functionals capture only about 50% of the interaction energy.[70] It is therefore not surprising that adding a dispersion term to mPW2-PLYP improves the performance of this functional. Even so, like all density functional methods, mPW2-PLYP-D underestimates the relative stability of the 280°-minimum.

The van der Waals/dispersion contributions computed by the DFT-D methods are displayed in Figure 7. Also shown is the df-LMP2/aug-cc-pVTZ correlation energy. Not surprisingly, the van der Waals term is smaller for mPW2-PLYP than for B3LYP, as the nonlocal perturbation term in the double-hybrid functional already accounts for part of the van der Waals energy. For both functionals, the van der Waals term is largest around ∼60°, where the contact between the C-terminus and the aromatic ring is closest (cf. Figure 3),

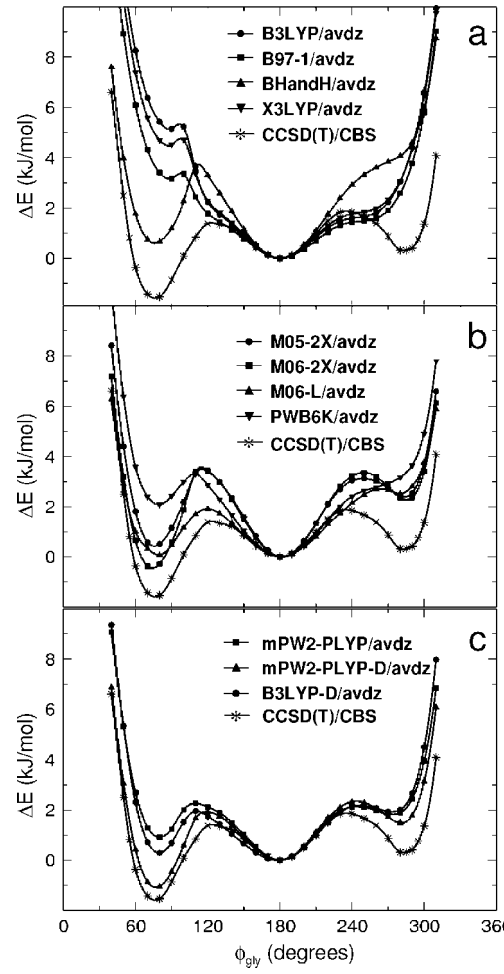

Figure 6. Potential energy profiles for rotation around the N(Gly)-C_α(Gly) bond computed with different density functionals and the aug-cc-pVDZ (avdz) basis set, using the M05−2X/6−31+G(d) set of geometries. The energy at $\phi_{Gly} = 180°$ was taken as the reference point for the relative energies. (a) Profiles computed with the hybrid functionals B3LYP, B97−1, BHandH, and X3LYP. (b) Profiles computed with the meta functionals PWB6K, M05−2X, M06−2X, and M06-L. (c) Profiles computed with mPW2-PLYP and B3LYP-D.

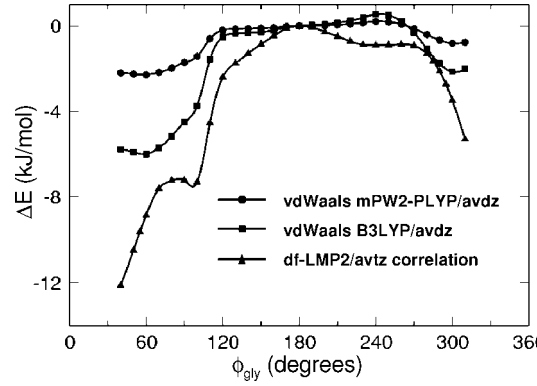

Figure 7. A comparison of the van der Waals contributions for B3LYP-D and mPW2-PLYP-D and the df-LMP2/aug-cc-pVTZ correlation contribution. The energy at $\phi_{Gly} = 180°$ was taken as the reference point for the relative energies.

and where the dispersion energy can be expected to be large. It should be noted, however, that the van der Waals

contributions cannot be interpreted as pure dispersion energy, but rather, the R^{-6} term in combination with the damping function corrects for DFT's general incorrect description of weakly bonded systems,[45,71] i.e. corrections other than for dispersion were absorbed in the fitted R^{-6} term coefficients and damping function parameters. However, the close resemblance of the MP2 correlation energy and the DFT-D van der Waals contributions indicate that the latter can be largely interpreted as dispersion. This is corroborated by recent work by Grimme et al.,[72] who used a partitioning of the interfragment MP2 correlation energy into electron pairs of different orbital type to study the intramolecular interaction in the same Tyr-Gly conformer as studied in the current work. It was shown that the MP2 correlation energy is mainly determined by the interfragment contribution, which can be interpreted as dispersion energy. Note that the different shapes of the HF, DFT-D dispersion, and MP2 correlation energy in the paper by Grimme et al. (specifically, the sharp peak at ~120° in the HF curve and the dips in the dispersion and correlation energy curves around 120°) are mainly due to the use of MP2/6−31+G(d) geometries in the study by Grimme et al., which, as shown above, exhibit very compact structures in the region around $\phi_{Gly} = 120°$.

4. Conclusions

We have tested a range of density functional theory methods for their ability to describe three minima along the ϕ_{Gly} profile of the Tyr-Gly conformer book4. These include one minimum with an extended glycine/C-terminus chain ($\phi_{Gly} = 180°$) and two more compact structures with a rotated C-terminus ($\phi_{Gly} = \sim 80$ and 280°). Previous work had shown that this is a demanding test for electronic structure methods: MP2 calculations with a medium-sized basis set miss the 180°-minimum because the potential energy surface is distorted by large intramolecular basis set superposition errors, whereas B3LYP misses the other two minima because of lacking dispersive interactions. Potential energy curves as a function of ϕ_{Gly} were compared to an estimated CCSD(T)/CBS reference profile. These calculations employed geometries optimized with M05−2X/6−31+G(d) for fixed ϕ_{Gly} values between 40 and 310°. We show here that the conventional hybrid functionals B3LYP, B97−1, BHandH, and X3LYP as well as the meta-hybrid PWB6K fail to predict all three minima; the meta-hybrid functionals M05−2X and M06−2X and the nonhybrid meta functional M06-L, on the other hand, do find all minima but underestimate the relative stability of the two with rotated C-terminus. The mPW2-PLYP double-hybrid functional and B3LYP-D (B3LYP augmented with an empirical dispersion term) slightly outperform the meta functionals by predicting barrier heights closer to those of the reference functional. However, also these underestimate the relative stability of the 80°- and 280°-minima. The best performance is delivered by the most elaborate density functional theory method tested: the double-hybrid functional augmented by an empirical dispersion term (mPW2-PLYP-D). mPW2-PLYP-D predicts the relative stability of the 80°-minimum in very close agreement with the reference profile, though the relative stability of the 280°-minimum is still slightly underestimated, even when allowing for the projected overestimation of approximately 0.4 kJ/mol of the stability of this point by the CCSD(T) reference profile. Only M06−2X and mPW2-PLYP-D predict the correct order of stability of the three minima (80°-minimum most stable, 280°-minimum least stable). It should be noted that the dispersion and correlation corrections in the mPW2-PLYP-D method only very slightly increase the computational cost: in the single-point calculations we performed, ~90% of the CPU time was spent on the calculation of the mPW-LYP energy, ~10% on the MP2 correlation correction, and a negligible percentage on the dispersion correction.

The geometries optimized at fixed ϕ_{Gly} values were found to be much dependent on the level of theory used. MP2/6−31+G(d) calculations obtained more compact structures than B3LYP/6−31+G(d), particularly around $\phi_{Gly} = 130°$. As previous work had shown that the intramolecular BSSE is particularly large in this region,[2] the more compact structures predicted by MP2 are probably mainly a result of this error and to a lesser extent due to dispersion forces; both effects are largely missing in the B3LYP calculations. The M05−2X geometries used to create the potential energy profiles are more compact than the B3LYP geometries (as expected from the presence of dispersion) but do not show the sharp increase in compactness around 120−130° as exhibited by the MP2 structures (because of the much smaller BSSE in DFT calculations). The M05−2X geometries are expected to be the most accurate of the three sets of geometries.

The compact MP2 geometries around 130° are not favorable for B3LYP calculations, with the result that a peak around 130° appears in the B3LYP energy profile when the MP2 structures are used. This is probably caused by repulsive energy contributions due to conformational strain and/or repulsive interactions between close atoms in the more compact MP2 structures. The MP2 profile, on the other hand, is only very slightly affected by the choice of geometries. The insensitivity of the MP2 results to the compactness of the structures is probably because the larger repulsive energy contributions in the more compact structures are more than compensated by intramolecular dispersion and/or BSSE (mostly absent in the B3LYP calculations).

The current study highlights the difficulty of reliably describing flexible molecules where intramolecular interactions with a π-electron system can be anticipated. Such interactions are affected by intramolecular BSSE (rendering MP2 methods with small to medium-sized basis sets unsuitable) and intramolecular dispersion-type interactions (providing a challenge for DFT methods). The performance of several modern DFT methods to describe such systems is quite promising.

Acknowledgment. We gratefully acknowledge the Royal Society for their support under the University Research Fellowship scheme and EaStCHEM for computational support via the EaStCHEM Research Computing Facility.

Supporting Information Available: The R_{CC} difference between B3LYP/6−31+G(d) and MP2/6−31+G(d) geometries and the energy penalty for computing the B3LYP and MP2 profiles using the geometries optimized with the

other method as a function of ϕ_{Gly} (Figure S1); potential energy profiles for rotation around the N(Gly)-C_α(Gly) bond computed with df-HF and df-LMP2 (Figure S2); Cartesian coordinates of the structures optimized at fixed ϕ_{Gly} angles using M05−2X/6−31+G(d) (Table S1); and total energies of the Tyr-Gly conformer book4 at fixed ϕ_{Gly} values, computed at different levels of theory (Tables S2a-e, S3a-d, and S4a-b). This material is available free of charge via the Internet at http://pubs.acs.org.

References

(1) Steiner, T.; Koellner, G. *J. Mol. Biol.* **2001**, *305*, 535–557.

(2) Holroyd, L. F.; van Mourik, T. *Chem. Phys. Lett.* **2007**, *442*, 42–46.

(3) Shields, A. E.; van Mourik, T. *J. Phys. Chem. A* **2007**, *111*, 13272–13277.

(4) van Mourik, T.; Karamertzanis, P. G.; Price, S. L. *J. Phys. Chem. A* **2006**, *110*, 8–12.

(5) Toroz, D.; van Mourik, T. *Mol. Phys.* **2006**, *104*, 559–570.

(6) Werner, H.-J.; Manby, F. R.; Knowles, P. J. *J. Chem. Phys.* **2003**, *118*, 8149–8160.

(7) Schütz, M.; Hetzer, G.; Werner, H.-J. *J. Chem. Phys.* **1999**, *111*, 5691–5707.

(8) Hetzer, G.; Pulay, P.; Werner, H.-J. *Chem. Phys. Lett.* **1998**, *290*, 143–149.

(9) Hetzer, G.; Schütz, M.; Stoll, H.; Werner, H.-J. *J. Chem. Phys.* **2000**, *113*, 9443–9455.

(10) Dunning, T. H. *J. Chem. Phys.* **1989**, *90*, 1007.

(11) Kendall, R. A.; Harrison, R. J. *J. Chem. Phys.* **1992**, *96*, 6796.

(12) Hampel, C.; Werner, H.-J. *J. Chem. Phys.* **1996**, *104*, 6286.

(13) Pedulla, J. M.; Vila, F.; Jordan, K. D. *J. Chem. Phys.* **1996**, *105*, 11091–11099.

(14) Saebø, S.; Tong, W.; Pulay, P. *J. Chem. Phys.* **1993**, *98*, 2170–2175.

(15) Schütz, M.; Rauhut, G.; Werner, H.-J. *J. Phys. Chem. A* **1998**, *102*, 5997–6003.

(16) Valdés, H.; Klusák, V.; Pitoňák, M.; Exner, O.; Starý, I.; Hobza, P.; Rulíšek, L. *J. Comput. Chem.* **2008**, *29*, 861–870.

(17) Becke, A. D. *J. Chem. Phys.* **1993**, *98*, 5648–5652.

(18) Lee, C.; Yang, W.; Parr, R. G. *Phys. Rev. B* **1988**, *37*, 785–789.

(19) Hamprecht, F. A.; Cohen, A. J.; Tozer, D. J.; Handy, N. C. *J. Chem. Phys.* **1998**, *109*, 6264–6271.

(20) Becke, A. D. *J. Chem. Phys.* **1997**, *107*, 8554–8560.

(21) Xu, X.; Goddard III, W. A. *Proc. Natl. Acad. Sci. U.S.A.* **2004**, *101*, 2673–2677.

(22) Becke, A. D. *J. Chem. Phys.* **1993**, *98*, 1372–1377.

(23) Sousa, S. F.; Fernandes, P. A.; Ramos, M. J. *J. Phys. Chem. A* **2007**, *111*, 10439–10452.

(24) Zhao, Y.; Schultz, N. E.; Truhlar, D. G. *J. Chem. Theory Comput.* **2006**, *2*, 364–382.

(25) Zhao, Y.; Truhlar, D. G. *J. Chem. Theory Comput.* **2005**, *1*, 415–432.

(26) Zhao, Y.; Truhlar, D. G. *J. Phys. Chem. A* **2005**, *109*, 6624–6627.

(27) Xu, X.; Goddard III, W. A. *J. Phys. Chem. A* **2004**, *108*, 2305–2313.

(28) Santra, B.; Michaelides, A.; Scheffler, M. *J. Chem. Phys.* **2007**, *127*, 184104.

(29) Èerný, J.; Hobza, P. *Phys. Chem. Chem. Phys.* **2005**, *7*, 1624–1626.

(30) Csontos, J.; Palermo, N. Y.; Murphy, R. F.; Lovas, S. *J. Comput. Chem.* **2008**, *29*, 1344–1352.

(31) Zhao, Y.; Truhlar, D. G. *J. Phys. Chem. A* **2005**, *109*, 5656–5667.

(32) Zhao, Y.; Truhlar, D. G. *Theor. Chem. Acc.* **2008**, *120*, 215–241.

(33) Zhao, Y.; Truhlar, D. G. *J. Chem. Phys.* **2006**, *125*, 194101.

(34) Zhao, Y.; Truhlar, D. G. *Phys. Chem. Chem. Phys.* **2005**, *7*, 2701–2705.

(35) Zhao, Y.; Tischenko, O.; Truhlar, D. G. *J. Phys. Chem. B* **2005**, *109*, 19046–19051.

(36) Zhao, Y.; Schultz, N. E.; Truhlar, D. G. *J. Chem. Phys.* **2005**, *123*, 161103.

(37) Zhao, Y.; Truhlar, D. G. *Acc. Chem. Res.* **2008**, *41*, 157–167.

(38) Zhao, Y.; Truhlar, D. G. *J. Phys. Chem. A* **2006**, *110*, 13126–13130.

(39) Valdés, H.; Spiwok, V.; Rezac, J.; Reha, D.; Albo-Riziq, A. G.; de Vries, M. S.; Hobza, P. *Chem. Eur. J.* **2008**, *14*, 4886–4898.

(40) Grimme, S.; Schwabe, T. *Phys. Chem. Chem. Phys.* **2006**, *8*, 4398–4401.

(41) Tarnopolsky, A.; Karton, A.; Sertchook, R.; Vuzman, D.; Martin, J. M. L. *J. Phys. Chem. A* **2008**, *112*, 3–8.

(42) Grimme, S. *J. Chem. Phys.* **2006**, *124*, 034108.

(43) Adamo, C.; Barone, V. *J. Chem. Phys.* **1998**, *108*, 664–675.

(44) Grimme, S. *J. Comput. Chem.* **2006**, *27*, 1787–1799.

(45) Grimme, S. *J. comput. Chem.* **2004**, *25*, 1463–1473.

(46) Antony, J.; Grimme, S. *Phys. Chem. Chem. Phys.* **2006**, *8*, 5287–5293.

(47) Piacenza, M.; Grimme, S. *J. Am. Chem. Soc.* **2005**, *127*, 14841–14848.

(48) Piacenza, M.; Grimme, S. *ChemPhysChem* **2005**, *6*, 1554–1558.

(49) Barone, V.; Biczysko, M.; Pavone, M. *Chem. Phys.* **2008**, *346*, 247–256.

(50) Schwabe, T.; Grimme, S. *Phys. Chem. Chem. Phys.* **2007**, *9*, 3397–3406.

(51) Hariharan, P. C.; Pople, J. A. *Theor. Chem. Acc.* **1973**, *28*, 213–222.

(52) Clark, T.; Chandrasekhar, J.; Spitznagel, G. W.; von Ragué Schleyer, P. *J. Comput. Chem.* **1983**, *4*, 294–301.

(53) Hehre, W. J.; Ditchfield, R.; Pople, J. A. *J. Chem. Phys.* **1972**, *56*, 2257–2261.

(54) Frisch, M. J.; Trucks, G. W.; Schlegel, H. B.; Scuseria, G. E.; Robb, M. A.; Cheeseman, J. R.; Montgomery, J. A., Jr.; Vreven, T.; Kudin, K. N.; Burant, J. C.; Millam, J. M.; Iyengar, S. S.; Tomasi, J.; Barone, V.; Mennucci, B.; Cossi, M.; Scalmani, G.; Rega, N.; Petersson, G. A.; Nakatsuji, H.; Hada, M.; Ehara, M.; Toyota, K.; Fukuda, R.; Hasegawa, J.;

Ishida, M.; Nakajima, T.; Honda, Y.; KitaoO.; Nakai, H.; Klene, M.; Li, X.; Knox, J. E.; Hratchian, H. P.; Cross, J. B.; Adamo, C.; Jaramillo, J.; Gomperts, R.; Stratmann, R. E.; Yazyev, O.; Austin, A. J.; Cammi, R.; Pomelli, C.; Ochterski, J. W.; Ayala, P. Y.; Morokuma, K.; Voth, G. A.; Salvador, P.; Dannenberg, J. J.; Zakrzewski, V. G.; Dapprich, S.; Daniels, A. D.; Strain, M. C.; Farkas, O.; Malick, D. K.; Rabuck, A. D.; Raghavachari, K.; Foresman, J. B.; Ortiz, J. V.; Cui, Q.; Baboul, A. G.; Clifford, S.; Cioslowski, J.; Stefanov, B. B.; Liu, G.; Liashenko, A.; Piskorz, P.; Komaromi, I.; Martin, R. L.; Fox, D. J.; Keith, T.; Al-Laham, M. A.; Peng, C. Y.; Nanayakkara, A.; Challacombe, M.; Gill, P. M. W.; Johnson, B.; Chen, W.; Wong, M. W.; Gonzalez, C.; Pople, J. A. *Gaussian 03, Revision E.01*; Gaussian Inc.: Wallingford, CT, 2004.

(55) *NWChem, Version 5.1*; High Performance Computational Chemistry Group, Pacific Northwest National Laboratory: Richland, WA 99352, U.S.A., 2006.

(56) Neese, F. *ORCA – an ab initio, density functional and semiempirical program package, 2.6, Revision 35*; University of Bonn: 2007.

(57) Vosko, S. H.; Wilk, L.; Nusair, M. *Can. J. Phys* **1980**, *58*, 1200–1211.

(58) Weigend, F.; Köhn, A.; Hättig, C. *J. Chem. Phys.* **2002**, *116*, 3175–3183.

(59) Groll, E.; Leininger, T.; Manby, F. R.; Mitrushchenkov, A.; Werner, H.-J.; Stoll, H. *Phys. Chem. Chem. Phys.* **2008**, *10*, 3353–3357.

(60) Hill, J. G.; Platts, J. A.; Werner, H.-J. *Phys. Chem. Chem. Phys.* **2006**, *8*, 4072–4078.

(61) Schütz, M.; Werner, H.-J. *Chem. Phys. Lett.* **2000**, *318*, 370–378.

(62) Schütz, M. *J. Chem. Phys.* **2000**, *113*, 9986–10001.

(63) Schütz, M.; Werner, H.-J. *J. Chem. Phys.* **2001**, *114*, 661–681.

(64) Werner, H.-J.; Knowles, P. J.; Lindh, R.; Manby, F. R.; Schütz, M.; Celani, P.; Korona, T.; Rauhut, G.; Amos, R. D.; Bernhardsson, A.; Berning, A.; Cooper, D. L.; Deegan, M. J. O.; Dobbyn, A. J.; Eckert, F.; Hampel, C.; Hetzer, G.; Lloyd, A. W.; McNicholas, S. J.; Meyer, W.; Mura, M. E.; Nicklass, A.; Palmieri, P.; Pitzer, R.; Schumann, U.; Stoll, H.; Stone, A. J.; Tarroni, R.; Thorsteinsson, T. *MOLPRO, a package of ab initio programs, version 2006.1*. http://www.molpro.net (accessed Sep 2008).

(65) Halkier, A.; Klopper, W.; Helgaker, T.; Jørgensen, P.; Taylor, P. R. *J. Chem. Phys.* **1999**, *111*, 9157–9167.

(66) Jurečka, P.; Hobza, P. *Chem. Phys. Lett.* **2002**, *365*, 89–94.

(67) Sinnokrot, M. O.; Sherrill, C. D. *J. Phys. Chem. A* **2004**, *108*, 10200–10207.

(68) Tsuzuki, S.; Honda, K.; Uchimaru, T.; Mikami, M.; Tanabe, K. *J. Am. Chem. Soc.* **2002**, *124*, 104–112.

(69) Riley, K. E.; Hobza, P. *J. Phys. Chem. A* **2007**, *111*, 8257–8263.

(70) Benighaus, T.; DiStasio, R. A.; Lochan, R. C.; Chai, J.-D.; Head-Gordon, M. *J. Phys. Chem. A* **2008**, *112*, 2702–2712.

(71) Bludský, O.; Rubeš, M.; Solán, P.; Nachtigall, P. *J. Chem. Phys.* **2008**, *128*, 114102.

(72) Grimme, S.; Mück-Lichtenfeld, C.; Antony, J. *Phys. Chem. Chem. Phys.* **2008**, *10*, 3327–3334.

CT800231F